Canadian Mineralogist
Vol. 21, pp. 41-58 (1983)

SPINEL ZONATION IN THE DE BEERS KIMBERLITE, SOUTH AFRICA: POSSIBLE ROLE OF PHLOGOPITE

JILL DILL PASTERIS

Department of Earth and Planetary Sciences & McDonnell Center for the Space Sciences, Washington University, St. Louis, Missouri 63130, U.S.A.

Abstract

Grains of zoned spinels from the well-mapped, multi-intrusion De Beers kimberlite pipe, Kimberley, South Africa, were studied optically and analyzed with an electron microprobe. Strict sampling control made it possible to show that spinel compositions and zoning trends are specific to individual kimberlite intrusions. In general, the compositions of kimberlitic spinel define a particular trend in the spinel prism, from the Al-rich to the Cr-rich regions at the base of the prism, then up toward the Fe^{3+}- or Ti-rich upper edge of the prism, commonly without great change in the $Fe^{2+}/(Fe^{2+} + Mg)$ ratio. No single kimberlite expresses the entire trend. The main root-zone intrusions of the De Beers kimberlite possess abundant grains of atoll spinel, with a core of chromite or titanomagnetite. The gaps in atoll spinels were once filled with Mg-pleonaste (Mg–Fe–Al-spinel), remnants of which are found only in contact zones adjacent to wallrock. Late-stage precipitation of high-Al, refractory spinel may have been triggered by the cessation of phlogopite precipitation during rise and fractionation of the kimberlite. Phlogopite is abundant in several of the root-zone intrusions, and commonly demonstrates multiple episodes of precipitation. An increase in $f(O_2)$ and other changes in the kimberlite melt subsequently caused breakdown and resorption of pleonaste everywhere in the pipe except in the contact zones, where the reaction did not go to completion.

Keywords: kimberlite, South Africa, root zone, spinel, phlogopite, atoll texture.

Sommaire

On a étudié optiquement et analysé à la microsonde électronique les spinelles zonés du pipe bien cartographié de De Beers (Kimberley, Afrique du Sud), à multiples venues kimberlitiques. Un contrôle strict de l'échantillonnage permet de prouver que composition et type de zonation sont caractéristiques de chaque venue. En général, de tels spinelles définissent une lignée caractéristique dans le prisme triangulaire des compositions qui part du pôle Al, va vers le pôle Cr à la base, et ensuite vers l'arête supérieure du prisme, dans une direction d'enrichissement en Fe^{3+} ou Ti, sans grand changement dans le rapport $Fe^{2+}/(Fe^{2+} + Mg)$. Aucune kimberlite ne montre à elle seule la lignée complète. Les phases intrusives principales de la zone profonde du complexe De Beers contiennent en abondance des spinelles à texture en atoll, avec noyau de chromite ou de titanomagnétite. Les lacunes de l'atoll étaient originellement remplies de pléonaste-Mg (spinelle Mg–Fe–Al), dont on trouve les vestiges dans les cristaux de spinelle au contact des roches encaissantes. La cristallisation tardive d'un spinelle alumineux réfractaire pourrait résulter de la fin de la cristallisation de la phlogopite lors de la mise-en-place et cristallisation fractionnée de la kimberlite. La phlogopite est abondante dans plusieurs de ces phases intrusives profondes, et montre dans plusieurs cas des stades multiples de cristallisation. C'est surtout à une augmentation de la fugacité d'oxygène dans le bain kimberlitique qu'on devrait attribuer la déstabilisation et la résorption du pléonaste partout sauf dans les zones de contact, où la réaction est restée incomplète.

(Traduit par la Rédaction)

Mots-clés: kimberlite, Afrique du Sud, zone profonde, spinelle phlogopite, texture en atoll.

Introduction

The mineralogy and petrology of numerous kimberlite intrusions are now documented in the literature (*e.g.*, Haggerty 1975, Mitchell 1978a, b, 1979, Mitchell & Clarke 1976, Mitchell & Meyer 1980, Boctor & Meyer 1979). The present study concerns the root zone of the well-mapped De Beers kimberlite diatreme in South Africa. It currently is being mined, and therefore was accessible for extensive horizontal and vertical sampling, in contrast to the more limited access available in many previous studies of kimberlites. The De Beers diatreme consists of several intrusions, which are recognizable by their field relations and their petrography.

The availability of fully documented samples (drill core and personally collected specimens) from several intrusions (facies) within a single

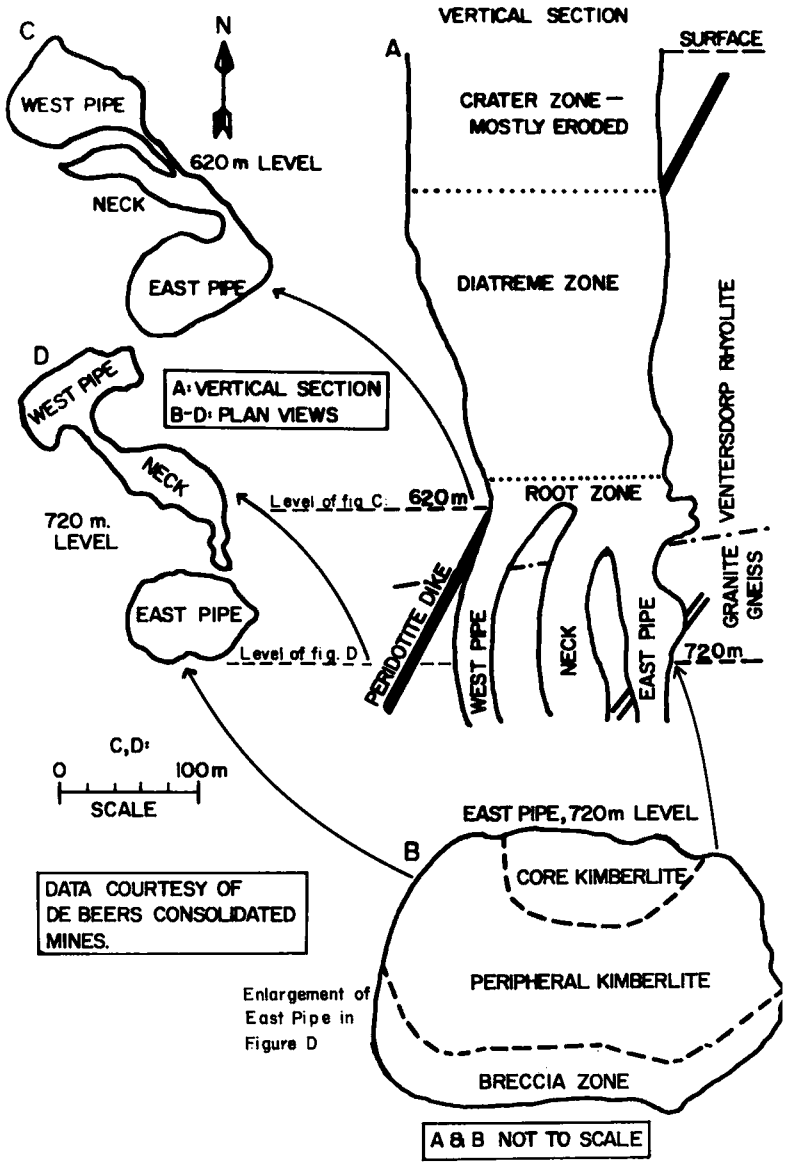

FIG. 1. Diagrammatic vertical section (A) and cross sections (B,C,D) of the De Beers pipe, Kimberley, South Africa. Each of the three major regions of the diatreme (C,D) probably represents at least one separate intrusion. Fig. 1B (enlargement of East Pipe in Fig. 1D): according to the De Beers geologists, the East Pipe consists of an earlier Peripheral Kimberlite, a later Core Kimberlite, and the Intrusion Breccia (part of the "Breccia Zone"). The Intrusion Breccia probably is not a separate intrusion, but rather Peripheral Kimberlite that has undergone extensive physical (and to some degree, chemical) interaction with the walls of the diatreme. Figure from Pasteris (1981), copyrighted by American Geophysical Union.

diatreme made it possible to compare petrological relationships among the kimberlite facies. The opaque oxide phases were chosen for particular study because they are the best-preserved

minerals of the rocks, and because their compositional variability makes them good indicators of changing conditions in the parent melt.

A major goal of this study was to determine the extent to which the opaque phases in kimberlite can be used as indicators of 1) differentiation processes within a kimberlite facies, and 2) genetic relationships among the facies.

Geology of the De Beers Kimberlite Complex

The De Beers kimberlite pipe is one of five major diatremes in the Kimberley district, South Africa. The diatremes are Cretaceous in age, about 90 Ma old (*e.g.*, U–Pb and Pb–Pb dating by Allsopp & Kramers 1977, Davis 1977). The basement rocks in the region are Precambrian granite and amphibolite gneiss. They are locally overlain unconformably by Ventersdorp volcanic rocks (~2300 Ma) and by more than 300 m of the sedimentary and volcanic rocks of the Karroo System (Carboniferous to Jurassic in age). The Precambrian and Ventersdorp rocks are the dominant wallrocks in the underground workings of the De Beers mine, where most of the samples examined in this study were collected.

The De Beers pipe has a geometry typical of many kimberlite pipes. It is dyke-like at depth, but expands abruptly into a funnel-shaped diatreme at about 2000 m below the original Cretaceous land surface (Fig. 1). Most samples analyzed in the present study come from the dyke-like root zone, which has the best-preserved igneous features of the intrusion.

The De Beers root zone has three major parts (Figs. 1 A,D,C) called the East Pipe, the West Pipe, and a Neck, each comprised of one or more separate intrusions. The East Pipe consists of two major intrusions, the Peripheral (earlier) and Core (later) kimberlites, plus several kimberlite dykes, a kimberlite sill, and a peridotite dyke. Field relations in the root zone suggest there were three or four major episodes of intrusion: Peripheral, followed by Core, followed by the Neck and the West Pipe (De Beers Geology Department). The Intrusion Breccia ("Breccia Zone" of Fig. 1B), which occurs in both the Neck and the East Pipe, is not considered a separate injection, but rather as kimberlite melt that has been affected by interaction with large volumes of wallrock. One of the reasons for comparing the compositional patterns of spinel among the different parts of the root zone is to determine if they too define the same number and physical extent of separate intrusions.

The East Pipe and Neck of the De Beers root zone were sampled by horizontal and vertical traverses across the 105-m level to the 729-m level (depths below the level of the present surface in the mine). Contact zones between the kimberlite and the wallrock were as well sampled as the middle of the intrusions. Drill-core samples (24) were studied from the 562-m level through the 720-m level of the West Pipe.

TABLE 1. SUMMARY OF PETROGRAPHIC FEATURES OF THE DE BEERS ROOT ZONE

Region	General Features	Degree of Serpentinization	Matrix Phlogo.	Pheno. Phlogo.	Spinel Abund. (A) & Preservation (P)	Spinel Zoning Type
West Pipe	well consolidated. coarse phlog. v. abund. Resembles Core K.	depth-depend., usu. at least partial.	v. abund., usu. colorless; if colored, R pleo	abund.; often altered rims; zoned (R core) or unzoned (N or R)	Low A. Poor P.	Type 2; atoll texture.
Core Kimberlite	more wallrk. incl. & serpentinization than Peripheral K.	variable, usu. moderate	abund., R pleo	some, altered	Low A. Poor P.	Type 2; atoll texture.
Peripheral Kimberlite	well consolidated, v. serpent. Fewer wallrk. incl. than Core K.	usu. partial.	some; pale color.	abund. at wallrk. contacts; zoned (R core) or unzoned (N or R).	Low A. P better than in Core. Grains largest at wallrk. contacts.	Type 2; atoll texture; some pleonaste remnants.
Neck Kimberlite	least altered & friable rock of body. Homogeneous & fine-grained.	variable, usu. partial.	in some samples.	abund. at wallrk contacts; altered elsewhere.	A: 1-3%. P better than elsewhere. Largest grains in pipe at contact.	Type 1, often in perovskite. Type 2; pleonaste abund. at wallrk; atolls.
Intrusion Breccia	fine-grained, basaltic. Some flow banding. Few wallrk incl.	variable, from none to complete.	rare.	abund., often well preserved.	A: 1-2%. P as in Neck. Largest grains at wallrk contact.	Type 1, often in perovskite. Type 2; pleonaste abund. at wallrk; atolls.
Dikes & Sill	v. friable; extreme hydration & carbonation. Coarse phlog abund.	usu. complete.	matrix & phenos form continuum.	abund.; zoned (R core) or unzoned (N or R).	Moderate A; usu. small.	unzoned titanomag & Type 1. Ilmenite incl. in titanomag.

abund = abundant; N = normal pleochroism; wallrk = wallrock
incl. = inclusions; pleo = pleochroism; R = reverse pleochroism; serpent. = serpentinized

Petrography of the De Beers Kimberlite

The different intrusions (facies) of the De Beers kimberlite can be distinguished on the basis both of their silicate and opaque oxide phases (Table 1). Throughout, olivine and phlogopite are the dominant phenocrysts, but they typically also occur in the matrix, which may comprise more than 50% of the rock volume. The matrix also contains calcite, serpentine, apatite, monticellite and opaque oxide phases. The major opaque oxide-minerals are spinel, rutile, perovskite and ilmenite, which together represent at most a few percent of the rock. A minor portion of the kimberlite consists of mantle-derived xenoliths and xenocrysts, particulary of garnet lherzolite and ilmenite.

In hand specimen, different kimberlite facies can be distinguished by color (hues of blue and green), friability, amount of crustal xenoliths, and degree of serpentinization and carbonation. All are porphyritic; some are obvious breccias. In thin section, further distinguishing features are the abundance and preservation of phlogopite, the abundance of segregations of calcite and serpentine, and zonation in the grains of spinel (Table 1).

Analytical Procedures

Analysis of spinel and phlogopite grains was carried out using the automated wavelength-dispersion MAC 400 electron microprobe at the Geophysical Laboratory, Washington, D.C. (Tables 2,3,4). The operating conditions for spinel analysis were 15 kV accelerating voltage, 50 nA beam current, 1–2-μm diameter beam-size, and 30 seconds counting time or 50,000 counts per element. The standards used are natural minerals, synthetic oxide phases and synthetic glasses. Because of the small size of the grains being analyzed, the elements Ca and Si were carefully monitored to ensure that matrix calcite and serpentine were not being excited by the beam. The data-reduction program is based on Bence–Albee correction procedures (Bence & Albee 1968, Albee & Ray 1970). Fe^{3+} and Fe^{2+} in the spinel (Tables 2, 3) were

TABLE 2. REPRESENTATIVE ZONED SPINELS FROM THE DE BEERS PIPE

	1 → 2		3 → 4		5 → 6		7 → 8		9 → 10		11 → 12		→ 13
MgO	10.46	4.23	13.83	18.96	11.61	13.14	11.56	12.88	17.88	19.89	21.42	13.26	12.74
FeO	20.90	29.83	25.90	11.39	19.55	27.04	21.59	27.69	12.21	9.64	9.67	15.23	31.02
MnO	0.94	1.01	0.70	0.46	0.96	0.91	0.64	0.69	0.91	0.80	0.67	0.57	0.77
NiO	0.21	0.37	0.21	0.00	0.03	0.11	0.21	0.15	0.14	0.17	0.21	0.19	0.16
CaO	0.07	0.18	0.36	0.50	0.40	0.41	0.27	0.17	0.24	0.36	0.28	1.14	0.18
Al_2O_3	11.32	0.54	9.00	38.43	4.14	6.13	5.18	7.33	5.87	8.75	9.61	8.65	5.52
Cr_2O_3	41.84	10.59	1.16	2.31	42.92	4.82	36.74	1.47	44.82	27.73	4.99	42.75	4.38
Fe_2O_3	8.87	45.35	29.93	22.42	10.36	28.04	14.15	30.49	11.11	23.57	43.02	11.46	25.12
TiO_2	4.91	6.75	17.21	3.95	7.71	18.24	8.65	17.56	8.09	8.93	10.23	5.01	20.70
SiO_2	0.09	0.44	0.26	0.39	0.01	0.00	0.19	0.23	0.24	0.25	0.97	0.26	0.17
TOTAL	99.61	99.38	98.56	98.81	97.69	98.84	99.18	98.66	101.51	100.09	101.07	98.52	100.76
Mg	0.514	0.233	0.682	0.800	0.595	0.658	0.582	0.644	0.841	0.928	0.983	0.652	0.630
Fe^{2+}	0.576	0.921	0.717	0.269	0.561	0.759	0.610	0.777	0.322	0.252	0.252	0.420	0.860
Mn	0.026	0.032	0.020	0.011	0.028	0.026	0.018	0.020	0.024	0.021	0.017	0.016	0.022
Ni	0.006	0.011	0.006	0.000	0.001	0.003	0.006	0.004	0.004	0.004	0.005	0.005	0.004
Ca	0.002	0.007	0.013	0.015	0.015	0.015	0.010	0.006	0.008	0.012	0.009	0.040	0.006
Al	0.440	0.024	0.351	1.281	0.168	0.243	0.206	0.290	0.218	0.323	0.349	3.336	0.216
Cr	1.091	0.309	0.030	0.052	1.166	0.128	0.982	0.039	1.119	0.686	0.121	1.114	0.115
Fe^{3+}	0.220	1.260	0.745	0.477	0.268	0.708	0.360	0.770	0.264	0.555	0.996	0.284	0.626
Ti	0.122	0.187	0.428	0.084	0.199	0.461	0.220	0.443	0.192	0.210	0.237	0.124	0.516
Si	0.003	0.016	0.009	0.011	0.000	0.000	0.006	0.008	0.008	0.008	0.030	0.009	0.006
TOTAL	3.00	3.00	3.00	3.00	3.00	3.00	3.00	3.00	3.00	3.00	3.00	3.00	3.00

1-2: Core Kimberlite; 720m level, near contact with Peripheral Kimberlite and basement gneiss; dark core (1) and light-colored rim (2).
3-4: Neck Kimberlite; 620m level, near contact with Ventersdorp wallrock; tan core (3) and black rim (4).
5-6: Intrusion Breccia; 720m level near Neck; chromite core (5) and tan rim (6).
7-8: West Pipe; 720m level; blue-gray core (7) and tan rim (8).
9-11: Peripheral Kimberlite; 720m level near contact with Core Kimberlite; gray core (9), edge of gray core (10), and outer rim (11). High Mg maintained throughout zoning.
12-13: Kimberlite Sill, blue core (12) and edge of core (13).

Note: colors refer to appearance in reflected light with oil-immersion objectives; Fe^{3+} calculated assuming stoichiometry of spinel (FERRIC program); in all the core-rim pairs and triplets above, the Mg and Al contents remain essentially constant or rise.

TABLE 3. MICROPROBE ANALYSES OF DE BEERS SPINELS WITH PLEONASTE RIMS

	1	2	3	4	5	6	7	8	9
MgO	19.94	13.36	13.83	14.27	20.08	20.32	20.39	20.12	20.00
FeO	9.51	24.75	25.90	22.60	10.36	9.74	10.54	10.76	9.98
MnO	0.84	0.82	0.70	0.71	0.30	0.29	0.32	0.29	0.28
NiO	0.09	0.16	0.21	0.29	0.00	0.03	0.07	0.02	0.00
CaO	0.59	0.30	0.36	0.23	0.43	0.30	0.30	0.18	0.34
Al_2O_3	8.96	6.76	9.00	15.93	47.16	49.32	48.22	46.10	45.80
Cr_2O_3	21.15	9.09	1.16	2.30	2.03	2.56	1.17	1.62	2.86
Fe_2O_3	27.62	27.68	29.93	29.54	15.80	14.38	15.51	16.22	16.20
TiO_2	9.83	14.86	17.21	12.66	3.18	2.36	3.09	3.46	2.72
SiO_2	0.14	0.71	0.26	0.40	0.00	0.00	0.25	0.17	0.23
TOTAL	98.67	98.49	98.56	98.93	99.34	99.30	99.85	98.95	98.41
Mg_{2+}	0.942	0.667	0.682	0.679	0.811	0.813	0.815	0.818	0.817
Fe^{2+}	0.252	0.693	0.717	0.603	0.235	0.219	0.236	0.245	0.229
Mn	0.023	0.023	0.020	0.019	0.007	0.007	0.007	0.007	0.006
Ni	0.002	0.004	0.006	0.007	0.000	0.001	0.002	0.000	0.000
Ca	0.020	0.011	0.013	0.008	0.012	0.009	0.009	0.005	0.010
Al	0.335	0.267	0.351	0.599	1.505	1.560	1.524	1.481	1.479
Cr_{3+}	0.530	0.241	0.030	0.058	0.043	0.054	0.025	0.035	0.062
Fe^{3+}	0.658	0.697	0.745	0.710	0.322	0.290	0.313	0.333	0.334
Ti	0.234	0.374	0.428	0.304	0.065	0.048	0.062	0.071	0.056
Si	0.004	0.024	0.009	0.013	0.000	0.000	0.007	0.005	0.006
TOTAL	3.00	3.00	3.00	3.00	3.00	3.00	3.00	3.00	3.00

Analyses #1-4: tan titanomagnetite cores of spinels with black pleonaste rims. #1: central region of Peripheral Kimberlite, 720 m level; #2-3: Neck Kimberlite, 620 m level, near contact with Ventersdorp wallrock; #4: Neck Kimberlite, 620 m level, about 4.5 m from contact.

Analyses #5-9: black, Mg-pleonaste spinel from 720 m level of Intrusion Breccia. Black spinels rim tan cores like those in Analyses #1-4.

Note: colors refer to appearance in reflected light with oil-immersion objectives; Fe^{3+} calculated assuming stoichiometry of spinel (FERRIC program).

TABLE 4. MICROPROBE ANALYSES OF DE BEERS PHLOGOPITE GRAINS

	1	2	3	4	5
Na_2O	0.03	0.00	0.06	0.26	1.17
K_2O	9.34	10.24	10.46	9.89	9.45
MgO	24.43	26.55	24.83	24.17	19.64
FeO	2.96	2.42	6.48	6.21	4.67
MnO	0.09	0.02	0.01	0.01	0.04
NiO	0.06	0.05	0.08	n.d.	n.d.
CaO	0.71	0.29	0.02	0.92	0.86
Al_2O_3	15.79	12.54	10.73	9.49	14.27
Cr_2O_3	0.02	0.01	0.11	0.29	1.65
TiO_2	1.63	0.52	0.61	0.83	3.99
SiO_2	38.04	42.03	43.19	41.98	40.38
Total	93.11	94.66	96.58	94.05	96.12
Na	0.002	0.000	0.008	0.037	0.162
K	0.861	0.924	0.943	0.919	0.854
Mg_{2+}	2.632	2.780	2.613	2.623	2.074
Fe^{2+}	0.178	0.141	0.381	0.378	0.277
Mn	0.004	0.000	0.000	0.001	0.003
Ni	0.002	0.002	0.004	n.d.	n.d.
Ca	0.053	0.021	0.000	0.077	0.065
Al	1.344	1.044	0.893	0.815	1.192
Cr	0.000	0.000	0.006	0.017	0.093
Ti	0.087	0.027	0.031	0.046	0.213
Si	2.748	2.971	3.050	3.056	2.861
Total	7.911	7.910	7.929	7.961	7.792

Cation values normalized to 11 oxygens; ideal formula is 8 cations per 11 oxygens. Analyses #1-3 from present study of De Beers kimberlite. Analyses #4 and 5 from Boettcher et al.'s (1979) data on the De Beers kimberlite, p. 175, sample Kb-5-1-A. #1: large, matrix phlogopite; sample DB19; Neck Kimberlite; 720m. level. #2: small, matrix phlogopite; sample DB31; Core Kimberlite: 742 m. level. #3: reverse pleochroic core of zoned phlogopite; sample DB428; kimberlite dike; 125 m. level. #4: reverse pleochroic core of zoned phlogopite. #5: normal pleochroic rim on grain #4.

calculated by assuming stoichiometry (FERRIC program, Geophysical Laboratory). Reconnaissance microprobe analysis was performed on phlogopite grains, using a broader beam ($\geq$ 5 μm) and a beam current of 40 nA. Many phlogopite grains are at least partly chloritized or serpentinized, as reflected in the oxide totals in Table 4.

Textural and Compositional Relationships Among the Spinel Minerals

Textural and zoning features

Spinel grains in the De Beers kimberlite occur in the following forms: individual grains in the groundmass, inclusions in perovskite, intergrowths with perovskite and ilmenite (but with no apparent reaction relationship), mantles on ilmenite macrocrysts, both as discrete grains and as massive reaction rims, and symplectic (fingerprint-like) intergrowths with silicate phases (Figs. 2–8). Spinel very rarely is seen as inclusions in olivine.

The spinel grains are relatively small ($<$ 35 μm) and were studied both in reflected and transmitted light with high-power oil-immersion objectives. They usually occur individually rather than in clusters, and they commonly exhibit resorption features.

Both unzoned titanomagnetite and zoned Cr-bearing spinel grains occur at De Beers, but zoned grains are more common. The two typical patterns of zoning from core to rim are: (1) chromite → (ilmenite) → titanomagnetite (Fig. 4), and (2) chromite/titanomagnetite → pleonaste (Mg–Fe–Al-spinel) → magnetite (Figs. 5,6). Grains of type 1 are found as inclusions in perovskite and individually in the matrix. However, type-2 grains always occur separately. This suggests that type-1 zoning represents an earlier sequence of precipitation, distinct from type-2 zoning.

In type-2 grains, the spinel core (euhedral to anhedral) commonly is separated from its lighter-colored outer rim(s) by a gap of several micrometres (Fig. 7). The term "atoll spinel" was applied by Mitchell & Clarke (1976) to such features in a Canadian kimberlite. In the De Beers atoll spinels, the core phase commonly is euhedral chromite or anhedral titanomagnetite. The outermost rim is so narrow ($\leq$ 5 μm) as to make electron-microprobe analysis difficult, but it clearly is rich in magnetite. The composition and optical properties of the "gap" resemble those of the fine-grained, calcite–serpentine mixture that comprises most of the kimberlite groundmass (Fig. 7).

The abundance, texture and composition of the opaque oxide phases are as characteristic of the different facies of kimberlite as are the primary and secondary nonopaque phases (Table 1). In general, type-1 and type-2 spinels occur in the Neck and Intrusion Breccia, whereas the West Pipe and East Pipe (Core and Peripheral kimberlites) contain only type-2 spinels. The West Pipe and Core kimberlites are recognized

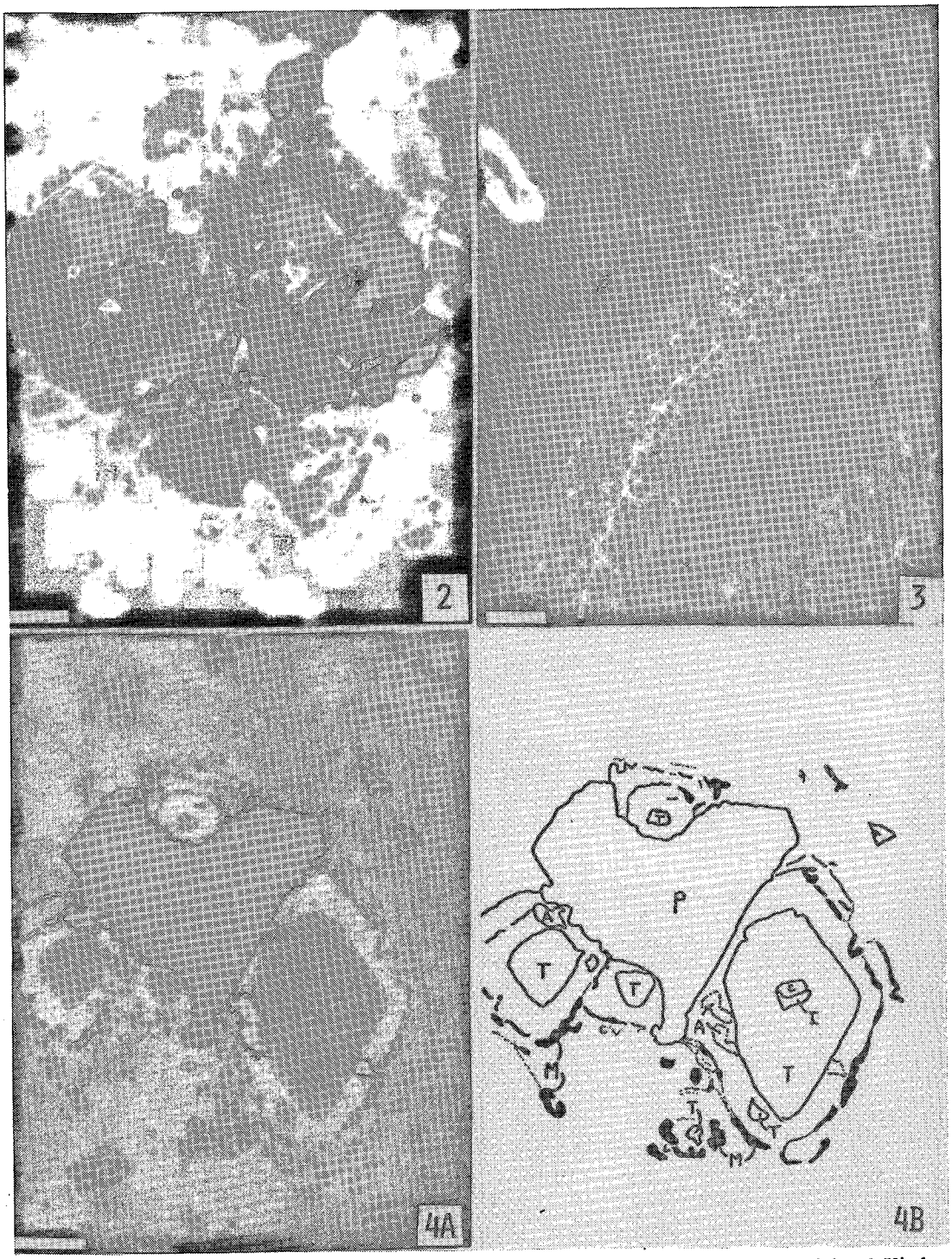

FIG. 2. Dark grey, subhedral titanomagnetite inclusions in light grey perovskite grain. Peripheral Kimberlite. Reflected light, oil-immersion objective. Scale bar 20 μm.

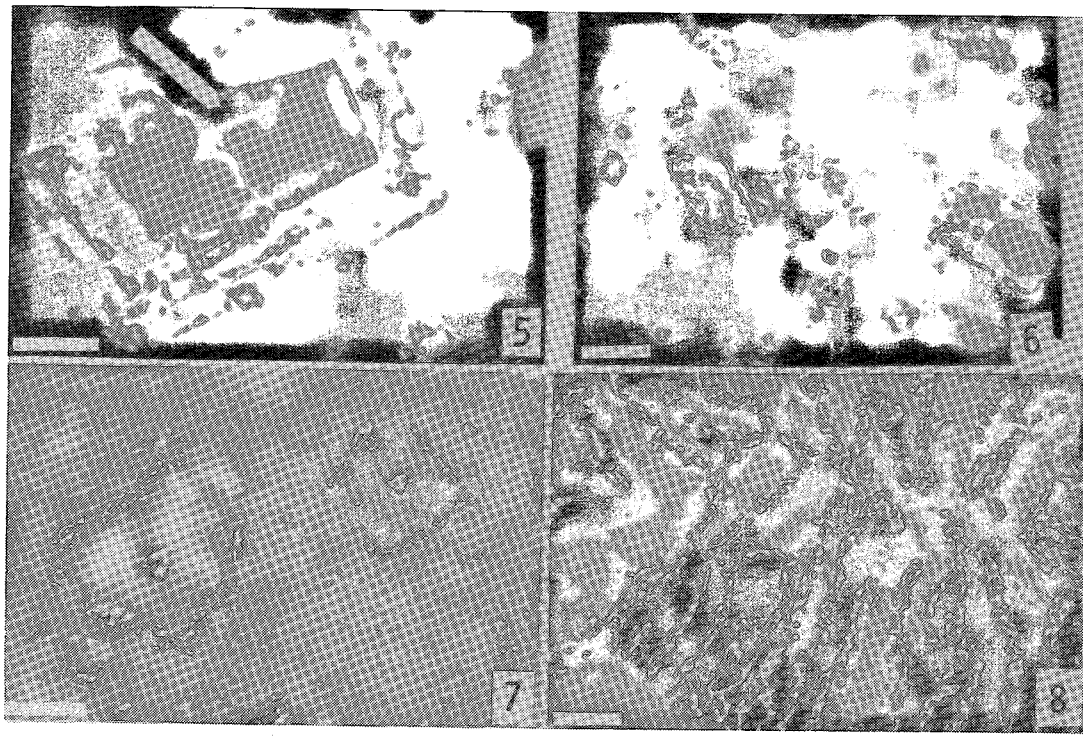

FIG. 3. Major phase (light grey), ilmenite, has been fractured and altered. Dark grey, highly titaniferous magnetite forms part of symplectic replacement zone. Small, highly reflecting inclusions in the ilmenite are sulfides. Neck Kimberlite. Reflected light, oil-immersion objective. Scale bar 20 μm.

FIG. 4A. Zoned atoll spinels attached to or partly enclosed in perovskite. 4B. Sketch. P perovskite, T titanomagnetite, M magnetite-rich spinel, C chromite, A anatase or perovskite. Neck Kimberlite. Reflected light, oil-immersion objective. Scale bar 10 μm.

FIG. 5. Zoned atoll spinel. Medium grey titanomagnetite, black (see arrow) Mg-pleonaste, white rims of magnetite-rich spinel. Core Kimberlite. Reflected light, oil-immersion objective. Scale bar 6 μm.

FIG. 6. Multirimmed grains of atoll spinel (left) and zoned spinel (right). In zoned grain, tan titanomagnetite core, Mg-pleonaste (black) inner rim, magnetite-rich (white) outer rim. Note partial resorption of both titanomagnetite and pleonaste. Note also juxtaposition of highly resorbed (left) and slightly resorbed (right) grains of atoll spinels. Neck Kimberlite. Reflected light, oil-immersion objective. Scale bar 20 μm.

FIG. 7. Atoll spinel with wide "gap" filled with kimberlite groundmass of serpentine and calcite. Note the small, euhedral chromite core and magnetite-rich spinel rim. Peripheral Kimberlite. Reflected light, oil-immersion objective. Scale bar 6 μm.

FIG. 8. Sympletic intergrowth of zoned spinel (chromite cores and magnetite-rich rims on the digits) and altered silicate. Such symplectite usually forms part of what appear to be mantle xenoliths. Core Kimberlite. Reflected light, oil-immersion objective. Scale bar 50 μm.

petrographically by the low abundance and poor preservation of their spinel grains; atoll grains (type-2 spinel with no pleonaste zone) are the most common. The kimberlite dykes and sill contain small single-phase euhedra of titanomagnetite and type-1 zoned spinel. Type-2 zoning and atoll spinel grains are absent in the dykes.

Compositional patterns

A principal feature of spinel grains in the De Beers and other kimberlites is a compositional discontinuity between the core phases, which are usually Cr-rich, and the rim phases, which are Ti-rich. This gap occurs both within grains and within kimberlite suites (*e.g.*, Hag-

gerty 1975); it also is apparent in magmatic ore deposits, in igneous complexes and, to a certain extent, in lunar rocks (*e.g.*, Haggerty 1976). The discontinuity may be due to a peritectic relationship between spinel and pyroxene (*e.g.*, Irvine & Smith 1969), to particular $f(O_2)$ conditions during crystallization of the melt (*e.g.*, Ulmer 1969, Hill & Roeder 1974), or to gaps in solid solution in the spinel system (*e.g.*, Muan *et al.* 1972).

Unfortunately, equilibrium coexistence of specific silicate and spinel phases cannot be inferred for the De Beers kimberlite nor, probably, for most kimberlitic pipes. Standard geothermometry and geobarometry techniques therefore, are not applicable. It is also difficult to prove equilibrium between specific grains of ilmenite and magnetite. Where the association does occur in kimberlites, the phases usually are too Mg-rich for the Buddington & Lindsley (1964) geothermometer – oxygen barometer to be applicable (Pasteris 1980a). One must therefore regard the zoned grains of kimberlitic spinel in themselves as indicators of magmatic trends. In the following paragraphs, spinel compositional patterns in the De Beers root zone are compared among the various facies and with patterns observed in other kimberlites.

Plots of microprobe-derived compositions show three distinct compositional groups on the spinel compositional prism (Figs. 9,10), namely (1) chromite (base of prism), (2) titanomagnetite (toward top of prism), and (3) Mg-pleonaste (almost exactly on the spinel–hercynite join). There is a wide spread in composition in groups 1 and 2, but not in group 3.

Two major compositional trends are evident in Figures 9 and 10. The first is a normal mag-

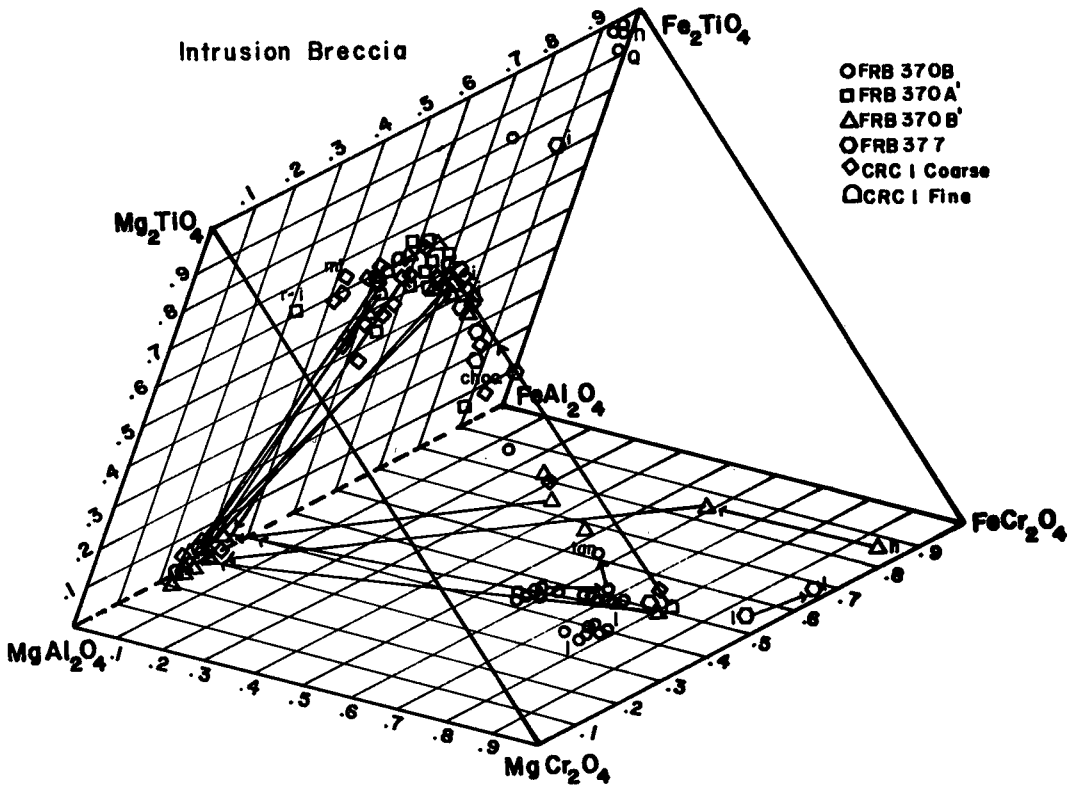

FIG. 9. Compositional plot for the spinels of the Intrusion Breccia; Fe^{2+} only plotted (Pasteris 1982). The lines and arrows represent core-to-rim zonation. Each type of symbol (*e.g.*, circle, square, triangle) represents a particular sample. All samples came from the 720-m level of the mine, except for FRB377, which came from the 620-m level (Fig. 1). Letter notations on the diagram refer to colors in reflected light and to unusual (and perhaps xenocrystic) grains (1,h,Q). Note the distinctive zonation pattern (type 2): chromite/titanomagnetite → Mg-pleonaste → magnetite; in some cases, not all three separate zones are present.

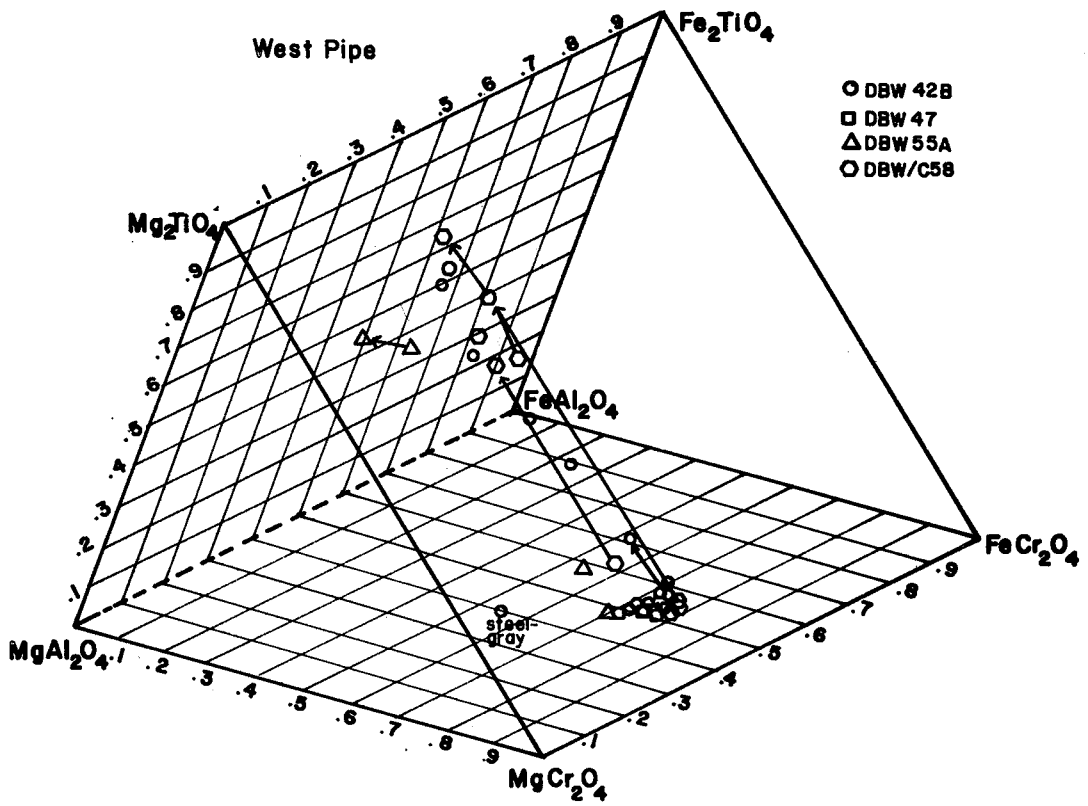

FIG. 10. Plot of compositions of spinel from the West Pipe. Tie lines and arrows connect core and rim of a zoned grain of spinel; each symbol type represents a particular drill-core sample. The specimens represent the following depth zones: DBW42B (620 m), DBW47 (660 m), DBW55A (710 m), DBW/C58 (720 m).

matic pattern, extending from chromite cores to titanomagnetite rims (Fig. 10). Between these end-members, data points are few, a feature that is common to many kimberlites and mafic complexes. The second trend appears unique to the De Beers pipe. In this case, titanomagnetite-rich cores are directly mantled by pleonaste rims (Fig. 9), and many of the titanomagnetite compositions appear to lie on a mixing line with pleonaste. However, the latter feature is not a function of integration of adjacent spinel zones by the electron-microprobe beam; many of the titanomagnetites plotted are *atoll* cores with no pleonaste rims present.

Although trend 1 (chromite → titanomagnetite) is represented throughout the pipe, trend 2 (titanomagnetite → pleonaste) is recorded only in the Intrusion Breccia and Neck. (Remnant pleonaste was optically identified in the Core and Peripheral kimberlites, but in grains too small for electron-microprobe analysis.)

Thus, compositional differences are evident in the spinel grains from different parts of the De Beers pipe (Table 2). The major distinctions are as follows: the presence or absence of trend 2, the extent (length in composition space) of the spinel compositional trends, the values of the $Fe^{2+}/(Fe^{2+} + Mg)$ ratios (FFM ratios), and the slope of the chromite–titanomagnetite tie-lines in compositional space. The typical range in FFM ratios for each part of the root zone is as follows: Core 0.20–0.45, Peripheral 0.20–0.55, Neck 0.20–0.55, Intrusion Breccia 0.20–0.80, West Pipe 0.40–0.55, and kimberlite Dykes and Sill 0.35–0.90. It is also clear from the data that spinel grains in close proximity to the wallrock commonly have compositions and textures distinctive from those in their host intrusions.

The apparently aberrant data points on Figures 9 and 10 (see captions) represent symplectites and other spinel grains derived from

mantle xenoliths. They are usually richer in Al and Mg than groundmass spinel in the kimberlite. Additional compositionally distinctive spinel grains in the kimberlite are those that mantle large crystals of ilmenite; they usually are richer in Ti and Fe than all other grains. There also is an optically distinct, salmon-colored (in reflected light), Ti-enriched spinel that is commonly present in veins between fragments of an ilmenite grain, or between an ilmenite and its massive perovskite rim (Fig. 3).

Spinel data were plotted on $Fe^{2+}/(Fe^{2+} + Fe^{3+})$ *versus* $Fe^{2+}/(Fe^{2+} + Mg)$ or FFF *versus* FFM diagrams (not shown; see Pasteris 1980a) to monitor how the increase in Fe^{2+} correlates with the change in total Fe. Because of the constraints that logically can be placed on the system under investigation, the FFF ratio probably can be used as an index of relative oxidation *within* the pipe. The iron ratios show distinctions among pipe facies and changes throughout differentiation. As FFM increases,

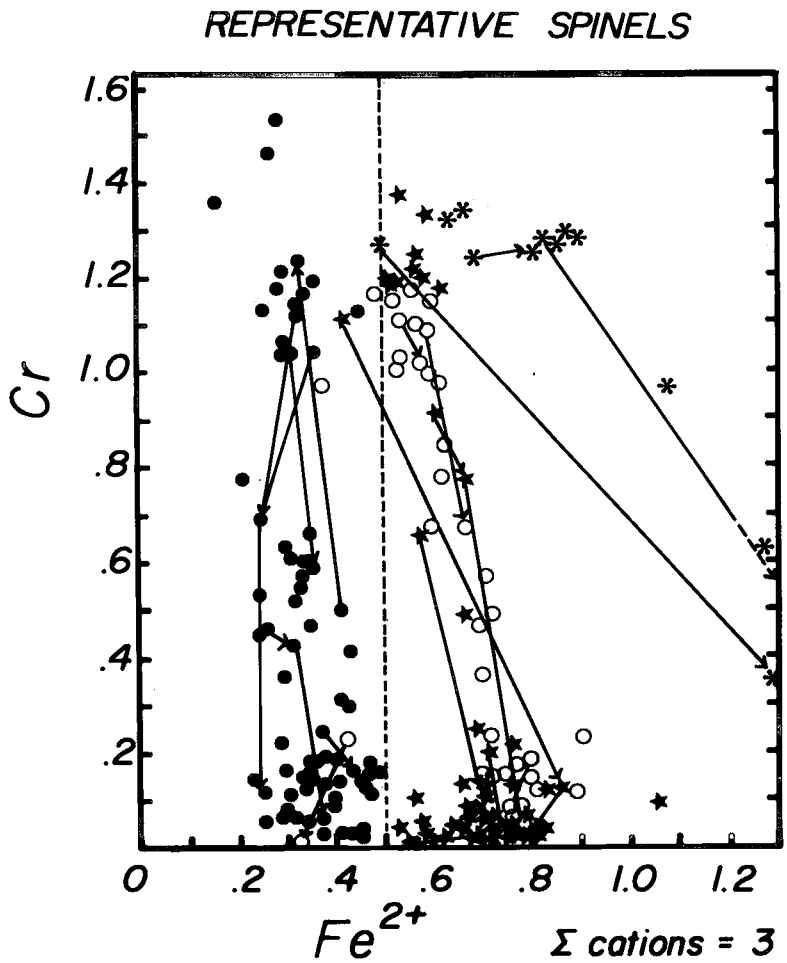

FIG. 11. Cr–Fe^{2+} plot of representative spinel compositions from each major region or intrusion in the De Beers pipe. For the sake of clarity, Mg-pleonaste compositions ($0.15<Cr<0.85$; $0.23<Fe^{2+}<0.27$) were not plotted on the graph. The vertical dashed line divides the main-stage Core and Peripheral kimberlites ($Fe^{2+}<0.5$) from the other facies in the De Beers pipe ($Fe^{2+}>0.5$). This method of plotting is described in Pasteris (1982). Solid circle: Core and Peripheral kimberlites, open circle: West Pipe, asterisk: peridotite dyke in the De Beers pipe, star: Neck Kimberlite, kimberlite dykes and sill.

FFF decreases in almost all cases. Thus, although Fe^{2+} increases with reference to Mg during fractionation, it increases more slowly than Fe^{3+}. Note here that Fe^{2+} and Fe^{3+} were calculated by assuming stoichiometry. Assuming that groundmass ilmenite was precipitated as spinel crystallized (Pasteris 1980b) and that the melt was oxygen-buffered, the negative slope of the spinel differentiation trend on an FFF–FFM plot may represent a decrease in temperature along a single $f(O_2)$ buffer.

In an effort to compare spinel compositions among the several kimberlite facies at approximately the same degree of fractionation, the FFF values were determined at selected FFM ratios. Chromite grains from the Core and Peripheral kimberlites have a higher content of Fe^{3+} than chromite from other parts of the pipe, an effect probably due to bulk-composition differences or perhaps to high $f(O_2)$.

As a first approximation, one can assume that all the De Beers intrusions have the same or a similar parent kimberlite melt. If this is true, the degrees of fractionation of the facies are indicated by the relative Fe-enrichment in their spinel compositions (Fig. 11). A plot of Cr *versus* Fe^{2+} (Fig. 11) in spinel indicates subtle differences between some facies, and shows a clear distinction between the Core and Peripheral kimberlites and all the other facies. The diagram indicates that the apparent sequence from least to most differentiated is Peripheral Kimberlite, Core Kimberlite, Neck, Intrusion Breccia, West Pipe, Kimberlite Dykes and Sill. This interpretation is in accord with the field evidence suggesting that the major episodes of intrusion at De Beers were the Peripheral, followed by the Core, followed by the Neck and the West Pipe. Spinel compositions also support the field interpretation that the contact kimberlite called the Intrusion Breccia was not a separate intrusion. It probably is Neck Kimberlite with a distinct cooling history. For instance, rapid, nonequilibrium cooling may have produced the strong Fe-enrichment recorded in Intrusion Breccia spinel grains.

Special Relationships in the Contact Zones

In the case of both phlogopite and spinel, not only do compositional and textural relationships differ among the kimberlite facies, but they also are strongly dependent upon the proximity to the wallrock. For instance, kimberlite in the contact region contains type-2 spinel grains with an intermediate zone of Mg-pleonaste, which, in turn, usually is rimmed by a thin magnetite-rich zone (Figs. 5,6). Away from contact regions in the same kimberlite facies, the intermediate zone of Mg-pleonaste usually does not exist. Instead there is a gap that gives rise to the atoll spinel grains described previously as a variation of type-2 zoning (see Fig. 7; *cf.* Mitchell & Clarke 1976).

Zoned spinel grains with Mg-pleonaste rims surrounding titanomagnetite cores occur almost exclusively in the Neck and the Intrusion Breccia, where the kimberlite is in direct contact with wallrock. Although Mg–Al-spinel rims are common here, one can see, in any given thin section from the two regions, not only fully preserved rims of pleonaste, but also atoll spinel grains that have only a partial pleonaste rim (Fig. 6).

The following textural evidence strongly suggests that Mg–Al-spinel rims originally were present in all the major root-zone facies. In the Intrusion Breccia and Neck, some grains with chromite or titanomagnetite cores have thick rims of pleonaste. In these cases, the pleonaste is subhedral and has no outer magnetite rim. More common in this region of the pipe are fragmentary patches of pleonaste around a chromite or titanomagnetite core. In such cases, a discontinuous, poorly developed outer rim of magnetite partly encloses the grain (Fig. 6). Only very rarely is (fragmentary) pleonaste identified in the Core and Peripheral kimberlites (Fig. 5). Such fragments usually are too small for quantitative analysis. On the other hand, in those samples (from the East Pipe, Neck, and West Pipe) in which pleonaste is not found, a black, translucent material occurs in some cases between the chromite core and magnetite rim. Microprobe analyses of the translucent material indicate variable quantities of Si, Ca and Ti (not titanite), but almost no Al. Much more commonly, this zone is filled with the same calcite–serpentine mixture that comprises the kimberlite matrix (supported by microprobe analysis). It is the latter grains of spinel that possess an atoll texture (Fig. 7).

Textural and compositional relationships thus suggest that in the main intrusions of the root zone, Mg–Al-spinel rims originally were present. Resorption of pleonaste is believed to have occurred in all but the contact kimberlite of the Neck and Intrusion Breccia.

The textural features of phlogopite phenocrysts also are related to their proximity to the wallrock. At increasing distances from the diatreme wall, phlogopite phenocrysts show enhanced development of thick, black rims (opaque to transmitted light) of a fine-grained, inhomo-

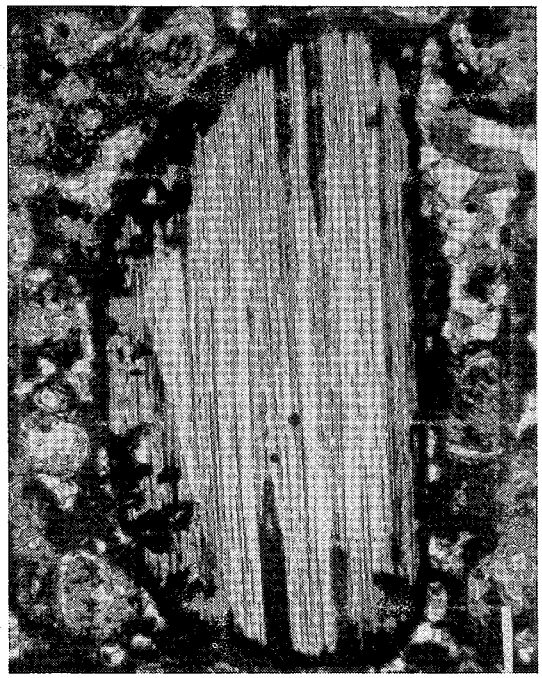

FIG. 12. Pleochroically zoned phlogopite that is possibly a mantle xenocryst (owing to large size). It is rounded (possibly due to physical attrition) and chemically altered to a black rind that extends inward along some cleavage planes. Matrix is calcite, serpentine and serpentinized olivine. Specimen DB44, kimberlite sill; transmitted light; scale bar 200 μm.

geneous product (Fig. 12). However, phlogopite phenocrysts are well preserved in the kimberlite nearest to the wallrock contacts.

GENETIC CONSIDERATIONS: POSSIBLE ORIGINS OF SPINEL ZONING

Spinels grains with a chromite core and a titanomagnetite rim can be explained by crystallization during normal magmatic differentiation. However, several questions arise concerning the pleonaste zones around titanomagnetite cores of spinel grains from certain regions of the kimberlite pipe: 1) Is the observed zonation in Al in spinel produced by magmatic precipitation? 2) How did late-stage enrichment occur in both Mg and Al, which is a reverse of the normal magmatic trend? 3) Why are pleonaste-rimmed spinel grains confined to certains regions of the pipe? 4) If resorption of pleonaste occurred elsewhere in the pipe, what was the reaction mechanism?

Several mechanisms were considered that might have produced the zoning sequence of titanomagnetite core, Mg-pleonaste inner rim, magnetite outer rim. Atomic-absorption spectroscopy, performed on bulk samples of kimberlite throughout the pipe, indicate no significant Al-enrichment due to wallrock contamination. Thus, the formation or preservation of pleonaste cannot be linked to the observable bulk-chemistry of the present rock.

The possibility was also considered that the zoning could reflect magma mixing [*cf.* Mitchell & Meyer (1980) for the Jos kimberlite dyke], *i.e.*, the introduction of a separate, somewhat Al-richer kimberlite melt caused precipitation of the pleonaste. One problem with this hypothesis is that the contaminant melt would have to be injected into only certain intrusions in the pipe. It also seems unlikely that the pleonaste-rimmed grains of spinel represent an entirely foreign suite of opaque phases; their size and the composition of their central chromite and titanomagnetite fractions match those of the other populations of spinel at De Beers.

A complex process of exsolution and recrystallization of an original aluminous titanomagnetite was considered as a possible origin for the zonation sequence titanomagnetite → pleonaste → magnetite. A ternary solvus exists in the two titanium-bearing systems $FeCr_2O_4$–Fe_2TiO_4–$FeAl_2O_4$ and $MgCr_2O_4$–Mg_2TiO_4–$MgAl_2O_4$, at least up to 1300°C (Muan *et al.* 1972); the solvus configuration is similar to compositional patterns in the De Beers spinel grains, as indicated in the triangular (Al, Cr, Fe^{3+} + 2Ti) plot in Figure 13. Although the compositions of the grains of zoned spinel at De Beers (Table 3) are compatible with a solvus relationship, the rimming textures are not. Furthermore, if titanomagnetite and pleonaste represent two limbs of a solvus, one would expect the two phases to be equally restricted in composition. However, Figure 13 shows this not to be true.

Although the widespread serpentinization in the De Beers kimberlite probably did not affect either the precipitation or the resorption of pleonaste, it was considered as a means of producing the thin outer rims of magnetite on the spinel. However, electron-microprobe analyses show that the pseudomorphic serpentine is approximately as iron-rich as unaltered olivine, obviating the need for expulsion of a magnetite component during serpentinization.

Owing to the relative geochemical immobility of Al, it appears to be a magmatic process that produced the zonation in Al. Because Al contents of the De Beers population of spinel not

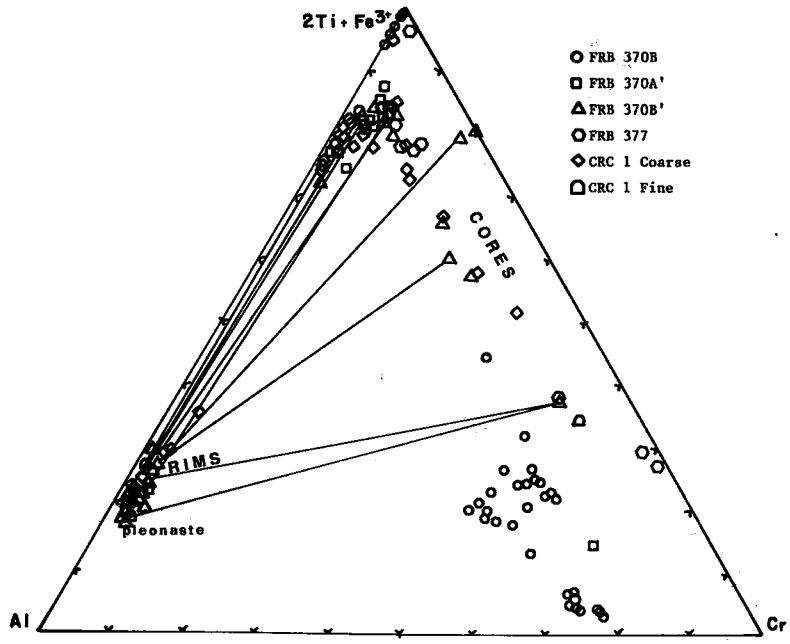

FIG. 13. Plot of spinel analyses from the De Beers pipe Intrusion Breccia. Tie lines connect core (Cr-, Ti-, Fe^{3+}-rich) and rim (Al-rich) in a grain. Symbols are the same as in Fig. 9. Note that Al contents are low and fairly constant except in the late-stage pleonaste, in which Al is high and relatively constant.

only are very low, but also almost invariant (Fig. 13) throughout their precipitation (pleonaste excepted), it seems reasonable that the Al content may have been controlled by coprecipitation of spinel and another aluminous phase.

TEXTURAL AND COMPOSITIONAL FEATURES OF PHLOGOPITE

Phlogopite occurs as phenocrysts, in the groundmass, as fine-grained rims on serpentine pseudomorphs after olivine, as part of garnet kelyphites, as mantle-derived inclusions (monomineralic or polymineralic), and as possible products of metasomatism (Table 1).

The largest phlogopite grains exceed 1 cm in length, but most grains classified as phenocrysts are in the range 0.3 to 2.0 mm. (Some of the largest grains are probably xenocrysts, but because phlogopite xenocrysts and phenocrysts cannot be distinguished optically, all large grains will be referred to as phenocrysts.) Many of the grains are zoned, consistently displaying reverse-pleochroic cores and normal-pleochroic rims (*cf.* Boettcher *et al.* 1979, Farmer & Boettcher 1981). For normal pleochroism in phlogopite, the relative coefficients of absorption are $\alpha < \beta \sim \gamma$; for reverse pleochroism, $\alpha > \beta \sim \gamma$. The reverse-pleochroic core comprises most of the phlogopite blade and usually is irregular to elliptical in outline, as though rounded by chemical reaction or physical abrasion. In the best preserved grains, the outline of each zoned crystal is euhedral despite the anhedral core (Fig. 14). Most of the blades have undergone alteration, the initial stages of which produce black rims opaque to transmitted light (Fig. 12). Electron-microprobe analyses show the black rims to be inhomogeneous. Some of them contain only 4–6 wt.% K_2O and only about 36 wt.% SiO_2 (*cf.* approximately 10 wt.% and 42 wt.%, respectively, in unaltered phlogopite), but more than 1 wt.% Na_2O. Representative compositions of the reverse-pleochroic core and normal-pleochroic rim of a large phlogopite blade appear in Table 4.

Matrix grains of phlogopite typically range in length from 0.02 to 0.04 mm. It is difficult to find individual, unaltered matrix laths of phlogopite suitable for microprobe analysis. The data in Table 4 indicate a lack of coherent compositional distinctions among the optically

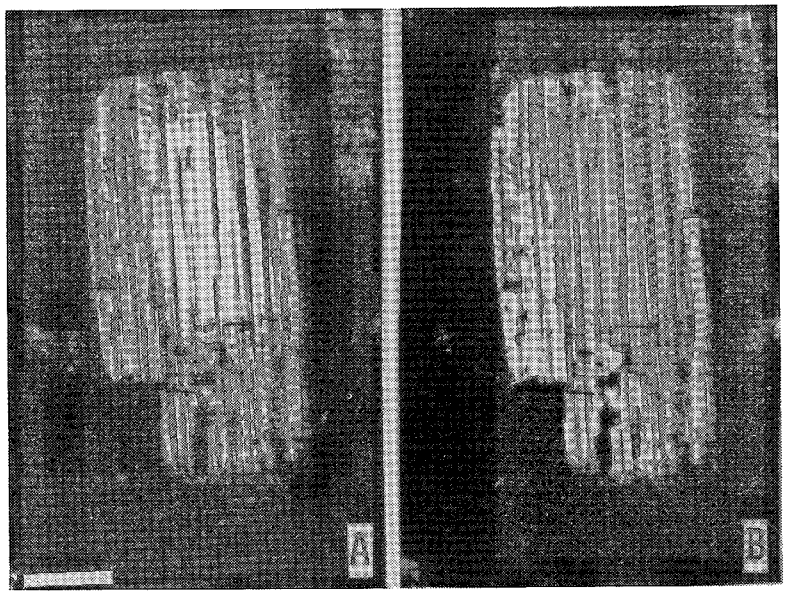

FIG. 14A,B: Pleochroically zoned phlogopite phenocryst, which is a common feature in the De Beers kimberlite. Polarizers rotated 90° between photographs A and B. Reverse-pleochroic core, normal-pleochroic rim. Transmitted light; specimen DB35B, kimberlite dyke; scale bar 100 μm.

distinguishable types of phlogopite. However, at least in some cases, groundmass phlogopite tends to be lower in Fe and Ti, and higher in Al and (in some cases) Mg than either reverse- or normal-pleochroic phlogopite phenocrysts. This represents a reversal of the normal magmatic trends toward late-stage enrichment in Fe and Ti. Groundmass blades in the major root-zone kimberlite facies characteristically are pale to colorless and, where colored, they exhibit reverse pleochroism and appear unzoned. The typical chronological sequence for phlogopite precipitation in the main root-zone (as distinct from the kimberlite dykes) appears to be (1) reverse-pleochroic phenocryst, (2) normal-pleochroic phenocryst, and (3) reverse-pleochroic or colorless groundmass phlogopite. The reversal in the pleochroic scheme and the compositional differences (Table 4) between the three defined types of phlogopite suggest a hiatus in crystallization between core and rim phenocrysts (cores commonly rounded) and between phenocryst and groundmass precipitation (*cf.* Farmer & Boettcher 1981).

In the kimberlite dykes and the sill that postdate emplacement of the main diatreme, phlogopite is very abundant. The grain-size distribution is not bimodal, however. Matrix and phenocryst grains form a continuum. The phlogopite grains may be zoned and have reverse-pleochroic cores, or they may be unzoned, in which case they have either reverse or normal pleochroism (Table 1).

PROPOSED RELATIONSHIP BETWEEN SPINEL AND PHLOGOPITE

Relationships observed in the De Beers kimberlite

Both spinel and phlogopite occur as zoned grains in the kimberlite groundmass. They are also the only major aluminous phases in the rock. Thus, possible correlations were investigated between the composition and abundance of all available generations of phlogopite and spinel (*cf.* Rimsaite 1971). Compositional variations in *phenocryst* phlogopite (for instance, its Cr content) do not appear to correlate with those in spinel. Furthermore, no correlation was found between the presence of groundmass phlogopite and the presence of rims of Mg–Al-spinel. Thus, the incorporation of Mg and Al into one of these two matrix phases did not preclude the formation of the other phase. As described in a previous section, however, there is a strong positive correlation between the *preservation* of Mg-pleonaste rims on zoned grains and the

preservation of phlogopite phenocrysts, both being enhanced at wallrock contacts. Phlogopite phenocrysts show increasing alteration away from the contact, but their serpentinized and chloritized pseudomorphs are readily recognized (and recorded in Table 1).

The positive correlation of the presence of these two phases appears to rule out late-stage Mg–Al-enrichment in the melt as primarily being due to the breakdown of phlogopite phenocrysts. However, another type of reaction relationship is possible between phlogopite and spinel. Precipitation of phlogopite depletes the melt in K, Mg, Al, Si and H_2O. The activity of one of these components may have decreased sufficiently to eliminate phlogopite precipitation temporarily, as demonstrated by the distinct generations of phlogopite in most regions of the root zone. If the activity of K or H_2O were the limiting factor, phases such as Fe–Ti-oxides could continue to crystallize. The concentration of Mg and Al eventually would rise in the melt, causing precipitation of other silicates and oxides by reactions such as the following:

$$\underset{\text{phlogopite}}{4KMg_3AlSi_3O_{10}(OH)_2} \rightarrow \underset{\text{forsterite}}{5Mg_2SiO_4} + \underset{\text{spinel}}{2MgAl_2O_4} + \underset{\text{melt}}{(2K_2O + 4H_2O + 7\ SiO_2)}$$

The simplified reaction indicates that decreases in K_2O and SiO_2 in the kimberlite melt could stabilize the assemblage forsterite + spinel + melt species over phlogopite.

As explained above, both the phlogopite and spinel relationships differ between the dyke and the main root-zone kimberlites (Table 1). These distinctions could be a function of differences in bulk composition, in pressure of emplacement, and in reactions with volatiles. Some mechanism that caused discontinuous precipitation of spinel and phlogopite apparently was active (perhaps episodically) in the root-zone intrusions, but not in the dykes. Textural evidence (Pasteris 1980a) indicates that, unlike the main intrusions in the root zone, the dyke kimberites did not undergo fluidization or any similar rapid evolution of a gas phase (separable from the melt). For instance, the spinel grains in the dyke are not rounded (*cf.* Mitchell 1978b) as are the titanomagnetite cores of the root-zone spinel (Fig. 6); large segregations of calcite and serpentine are more common in the dyke rocks, and much less rounding of large grains is evident in the dykes.

The histories of phlogopite and spinel development in the dyke and root-zone kimberlites apparently began to diverge after the precipitation of normal-pleochroic rims on reverse-pleochroic phlogopite phenocrysts. The following model is a possible history of subsequent processes. In the root-zone intrusions, volatile release or simple depressurization (both decreasing activity of H_2O) interrupted the precipitation of titanomagnetite and phlogopite. Mg and Al increased in concentration in the melt during the phlogopite hiatus, permitting pleonaste to precipitate. In the dykes, however, this disruption mechanism was not active. Continuous precipitation of titanomagnetite kept Fe^{3+} and Ti concentrations low in the melt, and *normal*-pleochroic (presumably low-Fe^{3+}) phlogopite continued to precipitate. As a consequence of continuous phlogopite precipitation, Mg and Al concentrations in the dyke melt never reached the saturation point of pleonaste.

Subsequent resorption of Mg-pleonaste in the root-zone intrusions is difficult to explain owing to its refractory nature. The ambient $f(O_2)$ may have risen during late-stage precipitation of spinel, causing oxidation of the initially ferrous pleonaste. The presence of at least a moderate $f(O_2)$ is supported by the magnetite component determined in the pleonaste (about 11 wt.% FeO and 15 wt.% Fe_2O_3 in preserved grains). An increase in the Fe^{3+} component could have shifted the pleonaste to a composition within the ternary extension of the known magnetite–hercynite solvus (Turnock & Eugster 1962), causing segregation of a magnetite$_{ss}$ and a spinel$_{ss}$ component. The Fe^{2+} component, which was oxidized to magnetite$_{ss}$, was precipitated "epitactically", whereas Mg and Al were resorbed by the remaining melt. This gave rise to the common atoll texture, and explains why the outer rim of magnetite occurs only where pleonaste is partly resorbed. The mechanism may be analogous to that documented by Price & Putnis (1979) in low-temperature, apparently non-equilibrium oxidation–exsolution of pleonaste granules associated with titanomagnetite.

Possible broader implications for kimberlite melts

Examination of these and other available data on spinel in kimberlites, especially those of Mitchell (1978a, b, 1979), leads to the conclusion that, broadly speaking, there is one general trend with several variations for kimberlitic spinel compositions (*cf.* Fig. 9). The initial trend is along the base of the spinel prism from the $MgAl_2O_4$-rich corner toward more Fe-rich chromite, with the addition of a small amount of Ti [seen in the Peuyuk and

Elwin Bay kimberlites, Northwest Territories (Mitchell & Clarke 1976, Mitchell 1978a) and in the Bellsbank kimberlite, South Africa (Boctor & Boyd 1979)]. Subsequently, Ti (and Fe^{3+}) increase, commonly without significant increase in the $Fe^{2+}/(Fe^{2+} + Mg)$ ratio. Compositions greatly enriched in the ulvöspinel–magnetite component can be attained in late-stage spinel or in rims on earlier Cr-rich spinel.

The following are several of the most obvious modifications to this general statement: 1) Entire compositional clusters of spinel data from one pipe commonly are displaced along the FFM axis of the prism diagram with respect to data points from other pipes. 2) In most cases, spinel compositions from a single pipe will not delineate the entire trend, *e.g.*, a) the initial phase may be an *Al-poor* chromite, as a Tunraq, N.W.T. and Kirkland Lake, Ontario (Mitchell 1978b, 1979) and at De Beers (this study), or b) the final Ti-enrichment may not be attained, as at Elwin Bay, N.W.T. (Mitchell 1978a), or c) *only* the final part of the trend may be represented, as at the Benfontein sill, South Africa (Dawson & Hawthorne 1973), Green Mountain, Colorado (Boctor & Meyer 1979), and in the Jos dyke, N.W.T. (Mitchell & Meyer 1980). 3) The late-stage spinel may become very rich in Fe^{3+} without much Ti enrichment, as in the massive micaceous kimberlite facies at Tunraq (Mitchell 1979) and in some atoll spinel rims at De Beers.

Of particular interest are the exceptions to the above trend, such as late-stage enrichment in Mg and Al in the pleonaste rim on spinel grains in some facies of De Beers (this study) and late-stage enrichment in Al over Cr in the spinel grains of the Kao kimberlite (Haggerty 1975). By a reaction process, aluminous spinel compositions developed in garnet kelyphites in the Monastery pipe (Haggerty 1975). These variations attest to the sensitivity of spinel to changes in its environment during both primary precipitation and subsequent re-equilibration, and to the need to assess the extent of spinel–silicate interaction.

The relationships described above suggest that compositions of groundmass kimberlitic spinel can be used to distinguish different kimberlite intrusions of a pipe and perhaps to order them with respect to their age of emplacement. In very complex multi-intrusion diatremes like the Premier pipe, South Africa, this would be no small feat. The spinel compositions also offer a means of comparing and contrasting kimberlite pipes with respect to degree of fractionation.

Summary of Conclusions

From this study of kimberlitic spinel, it is clear that spinel compositions and textures differ systematically within a single pipe. With respect to the De Beers pipe, field relations and compositional patterns of the spinel are compatible with the hypothesis that the main kimberlite facies of the root zone represent successive intrusions from a single, fractionating parent melt at depth. The obviously later-injected kimberlite dykes and sill are more fractionated than the main root-zone facies. The dykes and sill may have arisen from a different parent than the main root-zone rocks, or may represent the late-stage residual liquid of the same parent kimberlite. Textural and compositional features of the kimberlite dykes and sill suggest that they, unlike the main root-zone intrusions, did not undergo fluidization.

It also appears, from the data in this study and others, that there may be a single trend defined by spinel compositions precipitating during normal differentiation of kimberlite. If so, it may be possible to place in sequential order the separate intrusions of multi-injection kimberlite pipes. It also may be possible to better compare kimberlites from different districts with respect to their degrees of fractionation. A better understanding of spinel compositional patterns is especially important in highly carbonated (secondarily replaced) kimberlite-like intrusions, such as those from Kansas and Missouri (Pasteris, unpubl. data), in which zoned spinel is the only primary phase remaining.

Evidence in the De Beers kimberlite suggests that the aluminum content of the melt was controlled over much of the interval of crystallization by the coexistence of phlogopite and low-aluminum spinel. During the rise of the kimberlite melt, phlogopite is believed to have become unstable, and much of the available aluminum partitioned into an aluminous spinel phase (pleonaste). Subsequent increase in $f(O_2)$ in the late-stage kimberlite melt caused breakdown of the pleonaste and precipitation of a magnetite-rich rim on the grains of residual spinel. The latter process produced the atoll texture characteristic of the spinel. In the De Beers pipe, Mg-pleonaste zones in the spinel are inferred to have formed initially throughout the body, wherever the atoll texture now is observed. However, pleonaste was preserved only in kimberlite directly adjacent to the wallrock, which is also the region of best preservation of phlogopite phenocrysts. Presumably the pleonaste and phlogopite breakdown reactions did not go to

completion here owing to rapid cooling.

The mechanism described above for the development of grains of atoll spinel is proposed specifically for the De Beers kimberlite. Cursory microscope observations of about 25 other kimberlites from North America and southern Africa suggest that the atoll texture in spinel is very common. However, it could be due to a variety of mechanisms. The only other kimberlite-like suite reported to have spinel with a titanomagnetite core and a Mg-pleonaste rim are the unusual extrusive rocks of the Igwisi Hills, Tanzania (Reid *et al.* 1975, Pasteris unpubl. data). At Igwisi, the spinel grains are much larger than those of the De Beers kimberlites. The pleonaste rims usually are preserved, but apparent resorption effects, including atoll textures, are observed. The above resorption mechanism is proposed for atoll spinel at De Beers because of the optically traceable, progressive disappearance of Mg-pleonaste throughout the kimberlite root-zone.

Acknowledgements

Much of this paper represents work done for a Ph.D. thesis at Yale University under the advisorship of Brian J. Skinner, Philip M. Orville, John V. Walther, and Robert J. Tracy. Electron-microprobe analyses were carried out at the Geophysical Laboratory, and a travel grant for field work was provided by the Carnegie Institution of Washington, D.C. Kimberlite samples were obtained personally by the author through the courtesy of the De Beers Geology Department, Kimberley, South Africa. To the individuals involved in the above organizations and to Roger Mitchell and an anonymous reviewer, who read earlier versions of the manuscript, the author expresses her sincere appreciation. However, she retains full responsibility for all opinions and interpretations expressed.

References

Albee, A.L. & Ray, L. (1970): Correction factors for electron-probe microanalysis of silicates, oxides, carbonates, phosphates and sulfates. *Anal. Chem.* **42**, 1408-1414.

Allsopp, H.L. & Kramers, J.D. (1977): Rb–Sr and U–Pb age determinations on southern African kimberlite pipes. *Second Int. Kimberlite Conf. (Santa Fe), Extended Abstr.*

Bence, A.E. & Albee, A.L. (1968): Empirical correction factors for the electron microanalysis of silicates and oxides. *J. Geol.* **76**, 382-403.

Boctor, N.Z. & Boyd, F.R. (1979): Petrology of kimberlite from the De Bruyn and Martin Mine, Bellsbank, South Africa. *Carnegie Inst. Wash. Year Book* **78**, 496-498.

——— & Meyer, H.O.A. (1979): Oxide and sulfide minerals in kimberlite from Green Mountain, Colorado. *In* Kimberlites, Diatremes, and Diamonds (F.R. Boyd & H.O.A. Meyer, eds.). Amer. Geophys. Union. Washington, D.C.

Boettcher, A.L., O'Neil, J.R., Windom, K.E., Stewart, D.C. & Wilshire, H.G. (1979): Metasomatism of the upper mantle and the genesis of kimberlites and alkali basalts. *In* The Mantle Sample: Inclusions in Kimberlites and Other Volcanics (F.R. Boyd & H.O.A. Meyers, eds.). Amer. Geophys. Union, Washington, D.C.

Buddington, A.F. & Lindsley, D. (1964): Iron–titanium oxide minerals and synthetic equivalents. *J. Petrology* **5**, 310-357.

Davis, G.L. (1977): The ages and uranium contents of zircons from kimberlites and associated rocks. *Carnegie Inst. Wash. Year Book* **76**, 631-635.

Dawson, J.B. & Hawthorne, J.B. (1973): Magmatic sedimentation and carbonatitic differentiation in kimberlite sills at Benfontein, South Africa. *Geol. Soc. Lond. J.* **129**, 61-85.

Farmer, G.L. & Boettcher, A.L. (1981): Petrologic and crystal-chemical significance of some deep-seated phlogopites. *Amer. Mineral.* **66**, 1154-1163.

Haggerty, S.E. (1975): The chemistry and genesis of opaque minerals in kimberlites. *Phys. Chem. Earth* **9**, 295-307.

——— (1976): Opaque mineral oxides in terrestrial igneous rocks. *In* Oxide Minerals (D. Rumble, III, ed.). *Mineral. Soc. Amer., Rev. Mineral.* **3**, Hg-101–Hg-300.

Hill, R. & Roeder, P. (1974): The crystallization of spinel from basaltic liquid as a function of oxygen fugacity. *J. Geol.* **82**, 709-729.

Irvine, T.N. & Smith, C.H. (1969): Primary oxide minerals in the layered series of the Muskox intrusion. *Econ. Geol., Mon.* **4**, 76-94.

Mitchell, R.H. (1978a): Mineralogy of the Elwin Bay kimberlite Somerset Island, N.W.T., Canada. *Amer. Mineral.* **63**, 47-57.

——— (1978b): Composition of spinels in micaceous kimberlite from the Upper Canada mine, Kirkland Lake, Ontario. *Can. Mineral.* **16**, 591-595.

——— (1979): Mineralogy of the Tunraq kimberlite, Somerset Island, N.W.T., Canada. *In* Kimberlites, Diatremes, and Diamonds (F.R. Boyd and H.O.A. Meyer, eds.). Amer. Geophys. Union, Washington, D.C.

——— & CLARKE, D.B. (1976): Oxide and sulfide mineralogy of the Peuyuk kimberlite, Somerset Island, N.W.T., Canada. *Contr. Mineral. Petrology* **56**, 157-172.

——— & MEYER, H.O.A. (1980): Mineralogy of micaceous kimberlite from the Jos Dyke, Somerset Island, N.W.T. *Can. Mineral.* **18**, 241-250.

MUAN, A., HAUCK, J. & LOFALL, T. (1972): Equilibrium studies with a bearing on lunar rocks. *Proc. 3rd Lunar Sci. Conf.* **1**, 185-196.

PASTERIS, J.D. (1980a): *Opaque Oxide Phases of the De Beers Kimberlite (Kimberley, South Africa) and Their Petrologic Significance.* Ph.D. thesis, Yale Univ., New Haven, Conn.

——— (1980b): The significance of groundmass ilmenite and megacryst ilmenite in kimberlites. *Contr. Mineral. Petrology* **75**, 315-325.

——— (1981): Kimberlites: strange bodies? *Amer. Geophys. Union Trans.* **62**, 713-716.

——— (1982): Representation of compositions in complex titanian spinels and application to the De Beers kimberlite. *Amer. Mineral.* **67**, 244-250.

PRICE, G.D. & PUTNIS, A. (1979): Oxidation phenomena in pleonaste-bearing titanomagnetites. *Contr. Mineral. Petrology* **69**, 355-360.

REID, A.M., DONALDSON, C.H., DAWSON, J.B., BROWN, R.W. & RIDLEY, W.I. (1975): The Igwisi Hills extrusive "kimberlites". *Phys. Chem. Earth* **9**, 199-218.

RIMSAITE, J. (1971): Distribution of major and minor constituents between mica and host ultrabasic rocks, and between zoned mica and zoned spinel. *Contr. Mineral. Petrology* **33**, 259-272.

TURNOCK, A.C. & EUGSTER, H.P. (1962): Fe–Al oxides: phase relationships below 1000°C. *J. Petrology* **3**, 533-565.

ULMER, G.C. (1969): Experimental investigations of chromite spinels. *Econ. Geol., Mon.* **4**, 114-131.

Received April 6, 1982, revised manuscript accepted July 5, 1982.